

## Supplementary Information

### Formation of dialysis-free Kombucha-based bacterial nanocellulose embedded in a polypyrrole/PVA composite for bulk conductivity measurements

Nadia Nirmal, Michael N. Pillay, Marco Mariola, Francesco Petruccione, Werner E. van Zyl\*

School of Chemistry and Physics, University of KwaZulu-Natal, Westville Campus, Durban, 4000, South Africa

CONTENTS	PAGE
Preparation of Nanocellulose from Bacterial Nanocellulose: Dialysis Method	2
<b>Figure S1</b> Set-up of copper plates in apparatus for PPy@BNCC/PVA analysis	2
<b>Figure S2.</b> A photograph showing the conductivity apparatus and set-up.	3
<b>Figure S3.</b> TEM image of an active SCOBY bacteria found in this study.	3
<b>Figure S4.</b> Size distribution curves representing BNCC (dialysis-free).	4
<b>Figure S5.</b> Size distribution curves representing BNCC (dialysis method).	4
<b>Figure S6.</b> The FT-IR spectrum of dialyzed BNCC sample.	5
<b>Figure S7.</b> FT-IR spectra for different PPy@BNCC samples.	6
Discussion of Figure S7.	7
<b>Figure S8.</b> Raman spectrum of dialyzed BNCC sample.	8
<b>Table S1.</b> Example of calculated mass, volume, and density of samples.	9
<b>Table S2.</b> Measured current/A for PPy@BNCC/PVA (dialysis-free).	10
<b>Table S3.</b> Measured current/A for PPy@BNCC/PVA (dialyzed method).	11

### Preparation of Nanocellulose from Bacterial Nanocellulose: Dialysis Method.

Followed the same procedure as described for the dialysis-free method described in the main text. After the 30 minute sonication step, the suspension was dialyzed to remove residual acid and hydrolysate of cellulose in the suspension whereby a dialysis sock was cut to size and the sample was filled in the tube. The result was monitored by checking the neutrality of the dialysate. After a five-day pH testing and water changing period, the water was measured to have a pH 6 and the dialysis ceased.

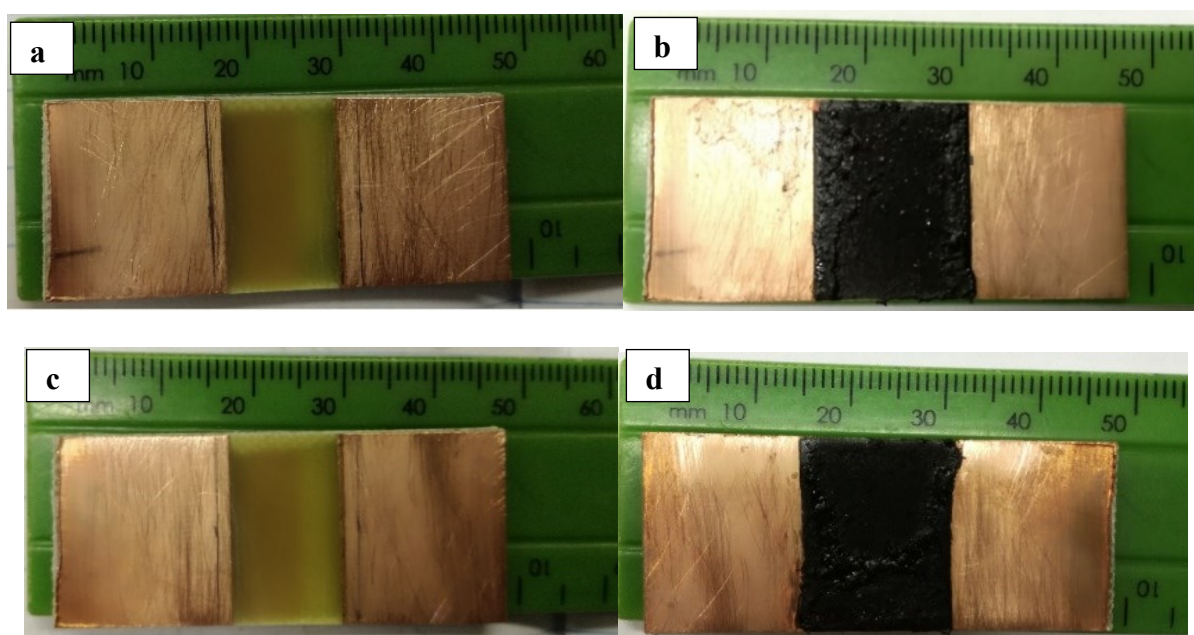


**Figure S1.** (a) The empty copper plate (b) the copper plate with PPy@BNCC/PVA from dialysis-free method (c) the empty copper plate (d) the copper plate with PPy@BNCC/PVA from dialysis method.

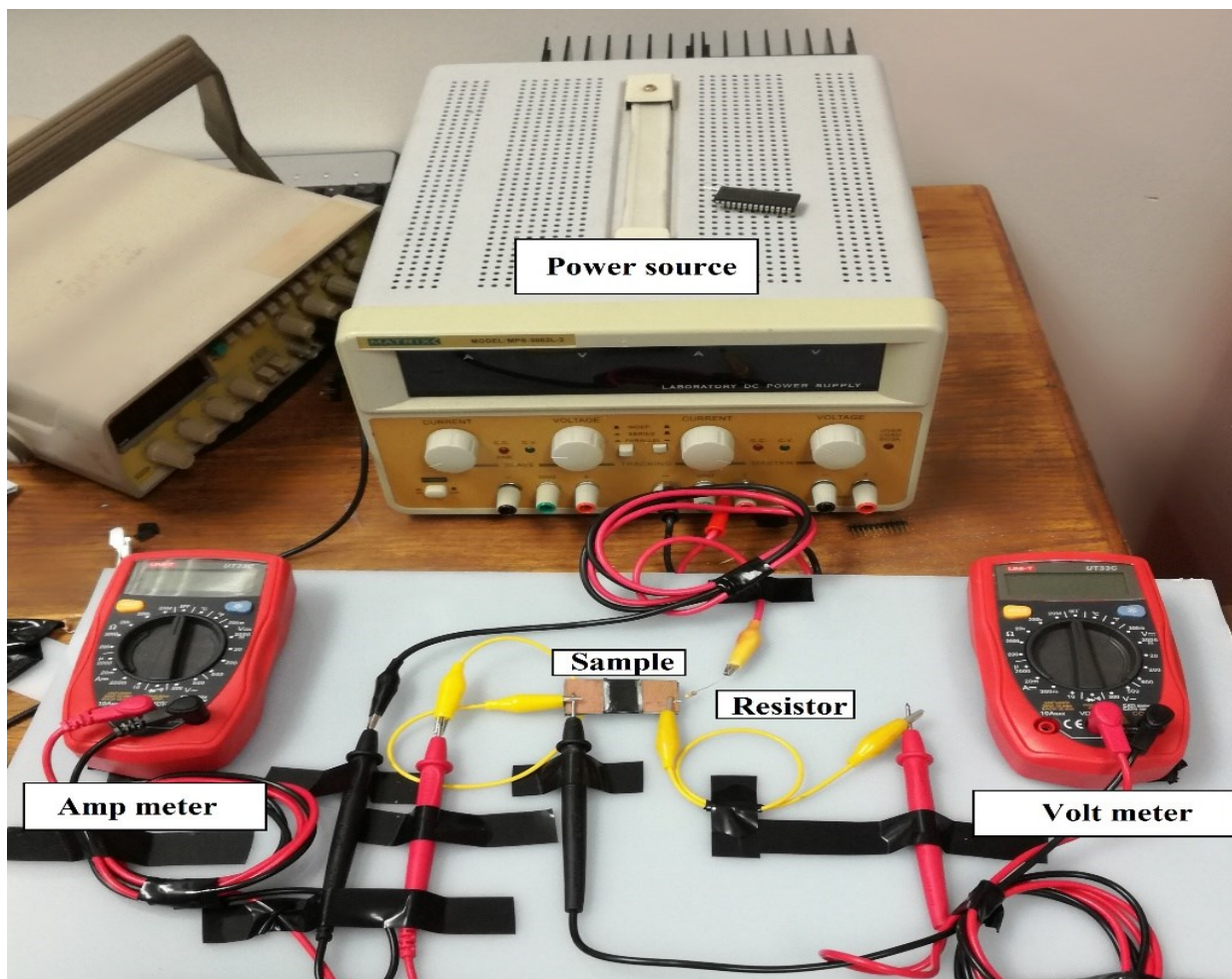


**Figure S2.** A photo showing the conductivity apparatus and set-up used in the study.



**Figure S3.** TEM image of an active SCOBY bacteria found in this study.

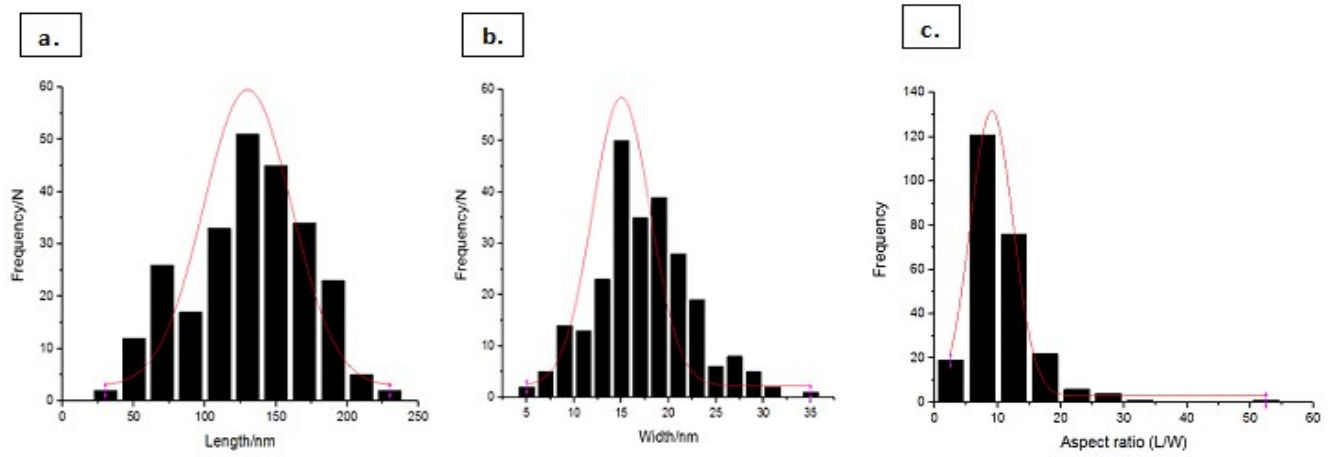


**Figure S4.** Size distribution curves representing the distribution of (a) average length, (b) width, and (c) aspect ratio of BNCC from dialysis-free method.

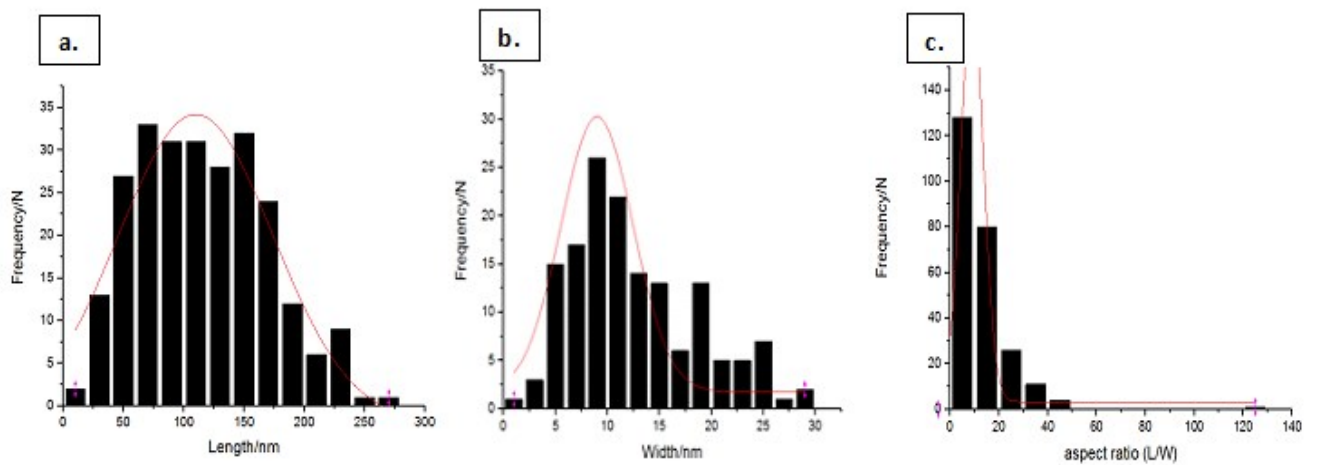


**Figure S5.** Size distribution curves representing the distribution of (a) average length, (b) width, and (c) aspect ratio of BNCC after dialysis.

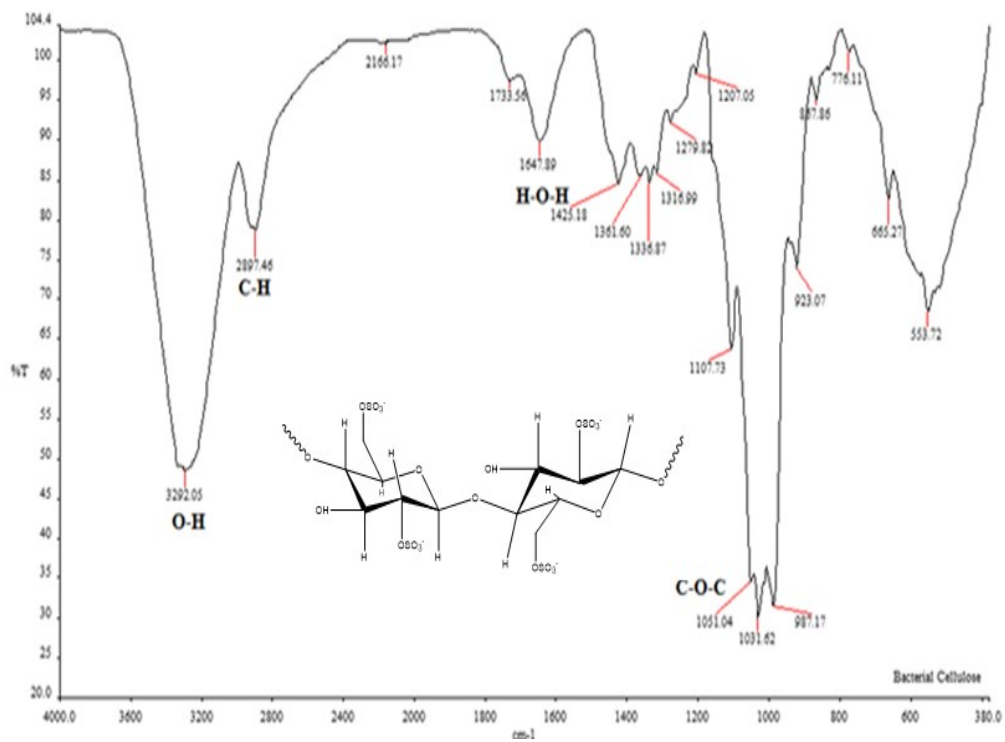


**Figure S6.** The FT-IR spectrum of dialyzed BNCC sample.

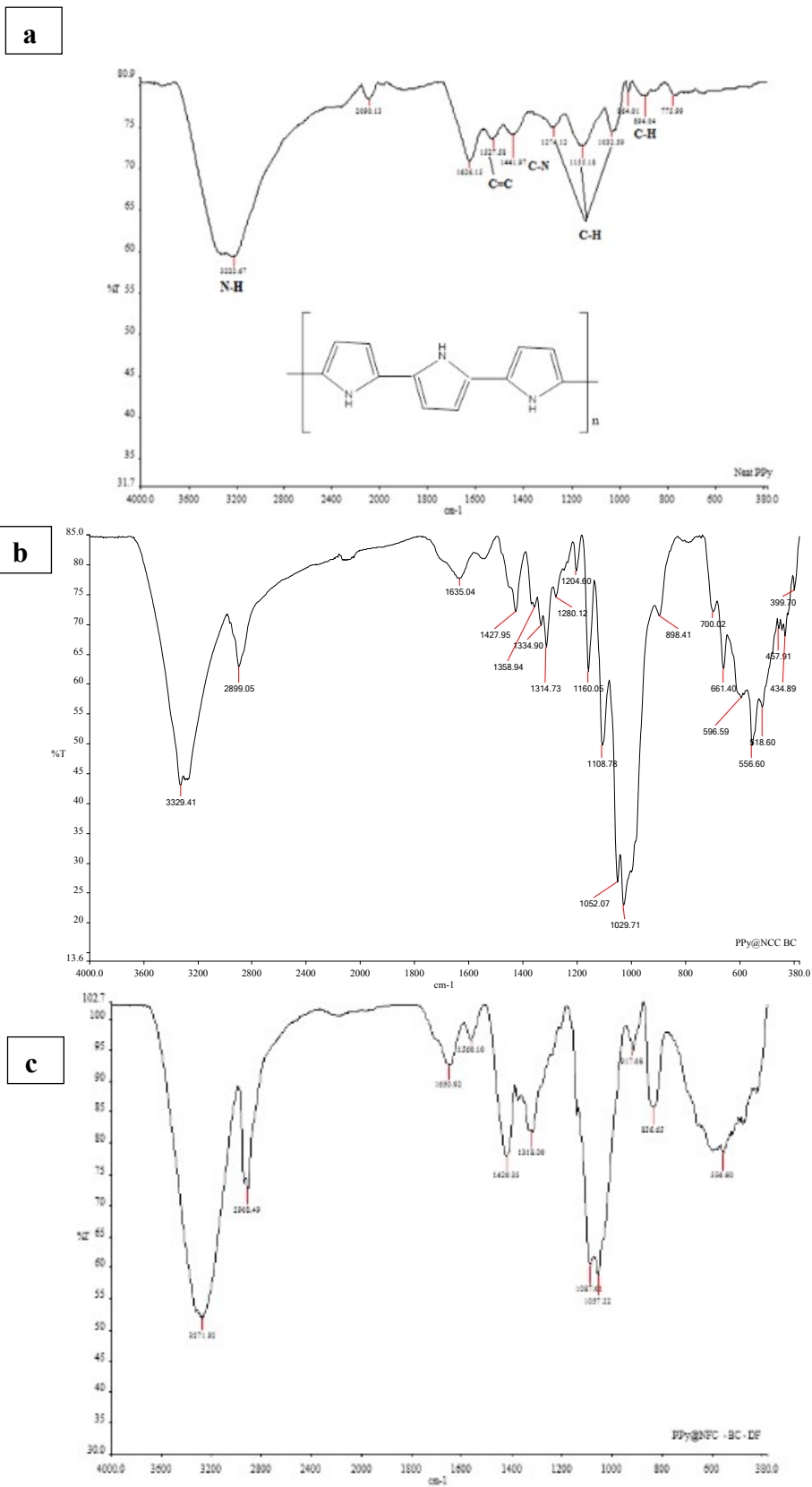


**Figure S7.** FT-IR spectra for (a) neat polypyrrole (b) PPy@BNCC (dialyzed) and (c) PPy@BNCC (dialysis-free).

FT-IR analysis was carried out to analyze the chemical structure of neat polypyrrole and PPy@BNCC nanocomposites. The characteristic bands of neat PPy is shown in Figure S7(a). The bands around 3222 and 1527  $\text{cm}^{-1}$  were assigned to the N-H stretching vibration and C-C ring stretching. The band at 1441  $\text{cm}^{-1}$  was assigned to the C-N stretching vibration in the pyrrole ring and bands at 1247, 1155, and 1032  $\text{cm}^{-1}$  to the C-H on-plane vibration, and the band at 894  $\text{cm}^{-1}$  to the C-H out-of-plane vibration.

The FT-IR for the dialyzed PPy@BNCC nanohybrid is shown in Figure S7(b) and dialysis-free method in Figure S7(c) and both exhibit very similar spectrums to that of neat PPy. However, all major peaks for PPy@BNCC have shifted wavenumbers with additional peaks attributed to the BNCC component, suggesting an interaction between PPy and nanocellulose. The FT-IR spectrum of PPy@BNCC nanocomposites appeared like a superposition of the FT-IR peaks of neat polypyrrole and nanocellulose. But the intensity of the O-H stretching band of BNCC and N-H stretching band of PPy decreased dramatically. On the other hand, peaks for BNCC and PPy in the nanocomposites shifted to lower wavenumbers compared to the neat BNCC and PPy. The results suggest that BNCC formed strong interfacial interactions with the polypyrrole, ascribed to the hydrogen bonding interaction between -OH and -NH moieties of BNCC and PPy, respectively.

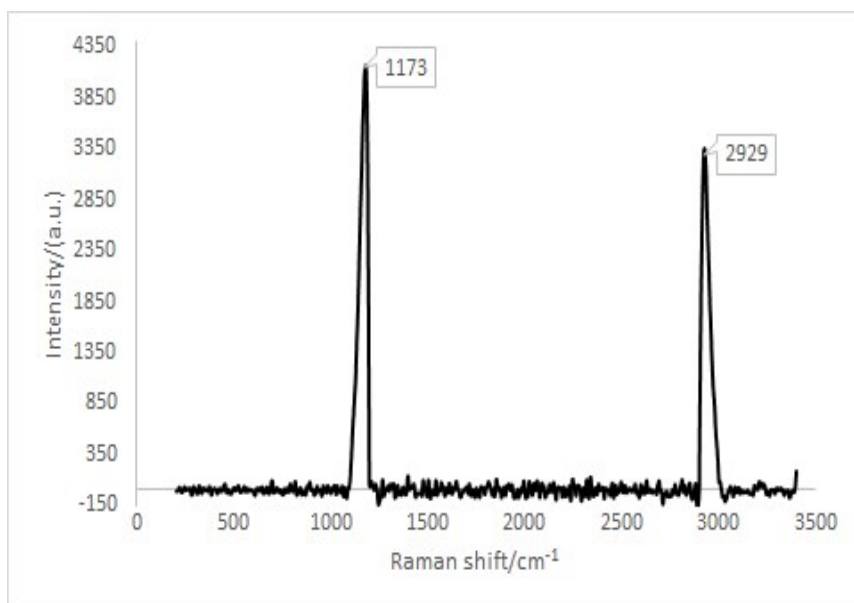


**Figure S8.** Raman spectrum of the dialyzed BNCC sample.



**Table S1.** Example of calculated mass, volume, and density of samples.

	<b>Dialysis method</b>	<b>Dialysis-free method</b>
	PPy@BNCC/PVA	PPy@BNCC/PVA
Mass of empty Cu plate/g	3.103	3.185
Mass of wet sample + Cu plate/g	3.182	3.262
Mass of wet sample/g	0.079	0.077
Mass of dry PPy@BNCC in PVA + Cu plate/g	3.140	3.221
Mass of dry PPy@BNCC in PVA/g	0.037	0.036
Mass of water/g	0.042	0.041
Volume of water/mL	0.042	0.041
Volume of PPy@BNCC in PVA/mL	0.208	0.209
Density of PPy@BNCC in PVA/g.mL <sup>-1</sup>	0.178	0.172
Volume of PPy@BNCC in PVA/mm <sup>3</sup>	208	209
Top surface area of film/mm <sup>2</sup>	347.314	364.660
Thickness of dry PPy@BNCC in PVA film/mm	0.599	0.573

**Table S2.** Measured current/A for PPy@BNCC/PVA (dialysis-free method), at applied voltage/V with calculated resistance.

<b>Voltage/V</b>	<b>Current/A</b>	<b>Resistance/<math>\Omega</math></b>
2.5	0.0016	1562.50
3	0.0018	1666.67
3.5	0.0020	1750.00
4.5	0.0024	1875.00
5.5	0.0025	2200.00
6.5	0.0029	2241.38
7.5	0.0033	2272.73
8.5	0.0036	2361.11
9.5	0.0040	2375.00
10.5	0.0043	2441.86
11.5	0.0047	2446.81
12.5	0.005	2500.00
13.5	0.0053	2547.17
14.5	0.0057	2543.86
15.5	0.0060	2583.33
16.5	0.0063	2619.05
17.5	0.0067	2611.94
18.5	0.0068	2720.59
19.5	0.0071	2746.48
20.5	0.0075	2733.33
	Average resistance/ $\Omega$	2339.94

**Table S3.** Measured current/A for PPy@BNCC/PVA (Dialyzed method), at applied voltage/V with calculated resistance.

<b>Voltage/V</b>	<b>Current/A</b>	<b>Resistance/<math>\Omega</math></b>
2.5	0.0010	2500.00
3	0.0011	2727.27
3.5	0.0013	2692.31
4.5	0.0016	2812.50
5.5	0.0019	2894.74
6.5	0.0022	2954.55
7.5	0.0025	3000.00
8.5	0.0028	3035.71
9.5	0.0031	3064.52
10.5	0.0034	3088.24
11.5	0.0036	3194.44
12.5	0.0039	3205.13
13.5	0.0042	3214.29
14.5	0.0045	3222.22
15.5	0.0047	3297.87
16.5	0.0050	3300.00
17.5	0.0052	3365.38
18.5	0.0055	3363.64
19.5	0.0058	3362.07
20.5	0.0058	3534.48
	Average resistance/ $\Omega$	3091.47